Increased Upstream Ionization due to Formation of a Double Layer

S. Chakraborty Thakur, Z. Harvey, I. A. Biloiu, A. Hansen, R. A. Hardin, W. S. Przybysz, and E. E. Scime

Department of Physics, West Virginia University, Morgantown, West Virginia 26506-6315, USA

(Received 9 October 2008; published 23 January 2009)

We report observations that confirm a theoretical prediction that formation of a current-free double layer in a plasma expanding into a chamber of larger diameter is accompanied by an increase in ionization upstream of the double layer. The theoretical model argues that the increased ionization is needed to balance the difference in diffusive losses upstream and downstream of the expansion region. In our expanding helicon source experiments, we find that the upstream plasma density increases sharply at the same antenna frequency at which the double layer appears.

DOI: 10.1103/PhysRevLett.102.035004 PACS numbers: 52.40.Kh, 52.20.−j, 52.25.Jm, 52.72.+v

Double layers (DLs) are narrow, local regions of strong electric field spatially isolated from plasma boundaries [1–3]. They often separate regions of plasma of different densities and temperatures and are an important mechanism for the acceleration of charged particles along magnetic fields in astrophysical plasmas. Recent experiments have demonstrated that current-free DLs form spontaneously in plasmas expanding in a diverging magnetic field. Retarding field energy analyzer (RFEA) probes [4,5] and nonperturbative laser-induced fluorescence (LIF) have been used to infer the existence of DLs through the detection of ion beams downstream of the expansion region. RFEA probes have also been used to measure the local plasma potential in the DL region; assuming that the measured acceleration of the bulk ion population results from the electric potential difference between the plasma potential and the grounded front aperture of the RFEA [1].

There are some intriguing aspects of these spontaneous DLs that are inconsistent with expectations for a classic DL. For example, the ion acceleration process occurs over many hundreds of Debye lengths [3] instead of the expected 10–50 Debye lengths [6]; the mean free paths of the plasma constituents appear to play a critically important role as the observations point to a low pressure threshold for DL formation; and recent reports of a threshold condition for the magnetic field strength in the source [7] suggest that DL formation also depends on the parameters of the distant plasma source.

The formation of DLs in a current-free plasma expanding in a divergent magnetic field was first predicted by Perkins in 1981 [8]. More recently, theoretical models have been developed for DLs in laboratory plasmas [9–11], in the solar corona [11] and at the boundary between the ionosphere and the auroral cavity [11]. In Ref. [10] a diffusion-controlled model describes formation of a DL in a plasma expanding from a small-diameter, dielectric source chamber to a large-diameter, conducting, expansion chamber; similar to our experimental configuration.

The diffusion-controlled model couples the dynamics of the particles in the non-neutral DL to the diffusive flows of the quasineutral plasma in the source and expansion chambers. As in a conventional DL model, the DL is embedded in a quasineutral plasma consisting of four groups of charged particles: thermal ions, monoenergetic accelerated ions flowing downstream, accelerated electrons flowing upstream and thermal electrons. To ensure that the DL is current-free, the model adds another group of counterstreaming electrons formed by reflection of accelerated electrons by the sheath at the insulated end wall of the source chamber. The potential difference across the DL is determined by the upstream and downstream particle balances. Since the upstream radius is smaller than the downstream radius, ionization by thermal electrons upstream is insufficient to balance the larger losses upstream. An additional source of upstream ionization becomes necessary and is provided by the accelerated group of electrons. In the model, the DL vanishes at very low pressures as the maximum ionization rate for the accelerated electrons upstream is insufficient to balance the excess upstream particle loss. At very high pressures, the system length becomes comparable to the energy relaxation length for ionizing electrons. Since electrons are heated upstream, the downstream ionizing electron density decreases at higher pressures. When the downstream and upstream ionization rates become equal to the corresponding particle loss rates, the additional ionization provided by the accelerated electrons is unnecessary and the DL vanishes.

Experiments in which the neutral pressure was varied demonstrated a pressure threshold for ion-beam formation [1–3] that is consistent with the predictions of the diffusion-controlled model. However, because the overall neutral pressure also changed in those studies, it was difficult to demonstrate that changes in the ratio of the upstream to downstream density (D_R) were solely a result of the formation of the current-free DL—a key prediction of the model. The substantially different magnetic field geometries in the recent study [7] that demonstrated a threshold in magnetic field strength for DL formation also made clear identification of the mechanism responsible for the observed change in D_R problematic.

In this Letter, we report observations of ion-beam formation downstream of an expanding helicon plasma which

depend only on the antenna frequency used to produce the helicon plasma. Key source parameters such as the forward and reflected rf powers, the neutral pressure, and the magnetic field geometry were kept constant. The plasma density, electron temperature and parallel ion velocity distribution function (IVDF) were measured both upstream and downstream of the expansion region.

The hot helicon experiment (HeLIX) vacuum chamber is a 61 cm long, Pyrex tube 10 cm in diameter connected to a 91 cm long, 15 cm diameter stainless steel chamber. The stainless steel chamber opens into a 2 m diameter, 4.5 m long expansion chamber. Ten electromagnets produce a steady state axial magnetic field of 0–1300 G in the source. Plasmas are created at pressures (with rf on) ranging from 0.1 to 100 mTorr. Rf power of up to 2.0 kW over a frequency range of 6–18 MHz is coupled into a 19 cm half wave, helical antenna to create the steady state plasma. Electron temperatures and densities in the source are measured with rf compensated Langmuir probes [12] at 50 cm downstream of the antenna (but upstream of the expansion region) and at 124 cm downstream of the rf antenna (at the same location as the LIF measurements [13]). The upstream LIF measurements were obtained 95 cm downstream of the rf antenna, just upstream of the expansion region.

For LIF measurements of the argon IVDF, the LIF laser system (see Ref. [14] for a complete description) is tuned to 611.662 nm (vacuum line) to pump the metastable Ar II $3d^2G_{9/2}$ state which then decays by emission at 460.96 nm. A typical LIF measurement consists of sweeping the frequency of a very narrow bandwidth laser through a collection of ions or atoms that have a thermally broadened velocity distribution function. As the laser frequency is swept over roughly 20 GHz, the fluorescent emission from the pumped excited state is collected and transported to a filtered photomultiplier tube (PMT). Since the PMT signal is composed of background spectral radiation, electron-impact-induced fluorescence radiation, and electronic noise, a lock-in amplifier is used to eliminate signals not correlated with the laser modulation. Ten percent of the beam is passed through an iodine cell for a consistent zero-velocity reference as well as compensation for laser drift [15].

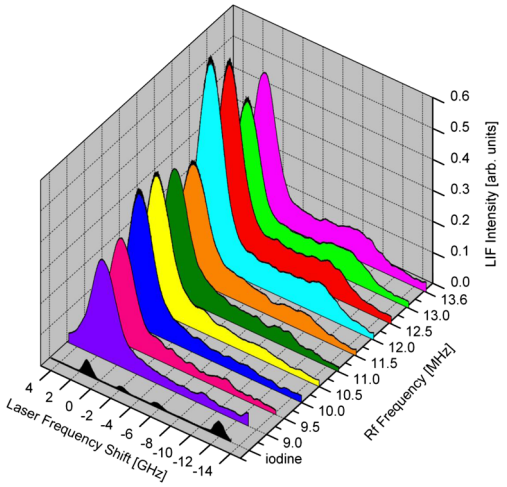

FIG. 1 (color online). LIF measurements of the downstream IVDF versus antenna frequency obtained 124 cm downstream of the antenna. The reference iodine line is also shown.

For IVDF measurements in a weak magnetic field, the LIF emission as a function of laser frequency is fit to a either a single or pair of drifting Maxwellian distributions

$$I_R(\nu) = I(\nu_o)e^{-mc^2(\nu-\nu_o)^2/2k_BT_i\nu_o^2} \quad (1)$$

where ν_o is the rest frame frequency of the absorption line, m_i the ion mass, and T_i the ion temperature. For magnetic fields of less than 100 G in the expansion region, Zeeman splitting of the two circularly polarized absorption lines is ignorable [16]. Upstream of the expansion region, only a single circular polarization of light is injected and therefore only one Zeeman split state is excited.

LIF measurements of the downstream IVDF versus laser frequency shift relative to the rest frame absorption line are shown in Fig. 1 for argon plasma at a rf power of 750 W, a magnetic field of 700 G, and a magnetic field of 50 G in the expansion region. With a constant flow rate of 3.6 sccm into the system, the pressures in the source and expansion regions were 0.2 mTorr and 0.05 mTorr, respectively. A negative shift in the frequency of the LIF line corresponds to ion flow towards the expansion chamber. The large amplitude peaks at small velocities are the background ion population. For antenna frequencies below 11.5 MHz, there is a strong background population and a population of ions extending across a wide velocity range. For helicon antenna frequencies of 12 MHz and higher, an ion beam appears at large, downstream directed, velocities. Based on fits to a pair of drifting Maxwellian distributions and after correcting the measured bulk flow speeds for the angle α of the downstream probe, the beam velocity decreases from approximately 9.0 km/sec at 12 MHz to 7.7 km/sec at 13.56 MHz.

For the same source parameters, the upstream and downstream plasma densities are shown in Fig. 2. There is gradual and continuous increase in the downstream plasma density with increasing antenna frequency, from 6×10^9 cm^{-3} at 9 MHz to 1×10^{10} cm^{-3} at 13.56 MHz. Upstream of the expansion region, there is a discontinuous increase in the measured density as the antenna frequency changes from 11.5 MHz to 12 MHz. This is the same frequency at which the downstream ion beam, and by implication the DL, appeared. With the DL present, the density increased to 2.6×10^{11} cm^{-3} from an average density of 0.85×10^{11} cm^{-3} without the DL; an increase of 210%. The corresponding increase in the downstream density was only 60%. It is important to remember that this increase in plasma density occurs without any change in the magnetic field geometry, pressure, forward rf power, or reflected rf power. If the upstream density increased be-

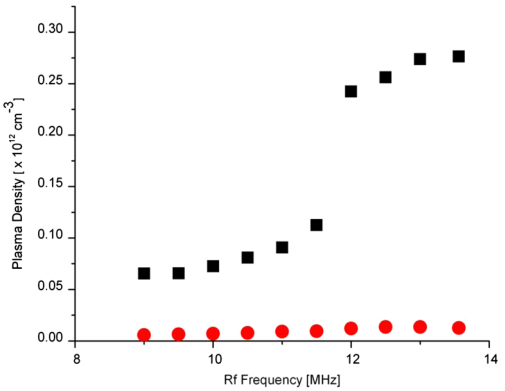

FIG. 2 (color online). Upstream (squares) and downstream (circles) density versus antenna frequency. The error bars are smaller than the size of the data points.

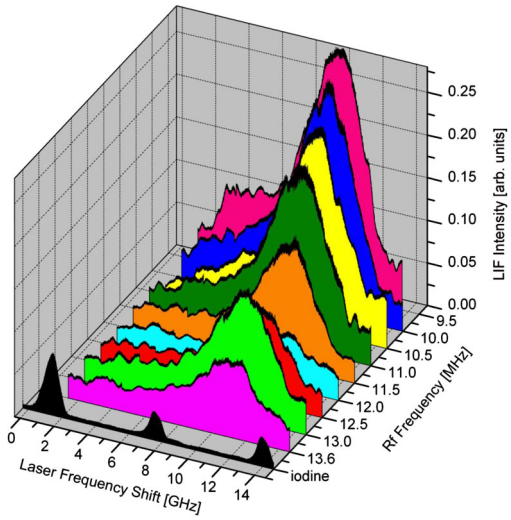

FIG. 3 (color online). LIF measurements of the upstream IVDF versus antenna frequency obtained 95 cm downstream of the antenna. The reference iodine line is also shown.

cause of improved confinement (perhaps through decreased transport) or improved rf energy absorption upstream, the downstream density should have increased by an identical ratio. The upstream density increase is also not a result of a significant change in the upstream density profile as no significant steeping of the upstream density profile was observed.

There is also distinct change in the upstream electron temperature at antenna frequencies above 12 MHz. The upstream electron temperature drops from 10.5 eV when the DL is not present to an average of 8.7 eV for antenna frequencies at which the ion beam is observed downstream. The downstream electron temperature is relatively constant at an average value of 7.9 eV for all rf frequencies. Again, if reduced Bohm losses to the wall (due to the decrease in electron temperature) were responsible for the increased upstream density, the downstream density should have increased by an identical factor of 210%.

To obtain sufficient signal-to-noise for LIF upstream, the source parameters were slightly changed. The magnetic field in the expansion region was decreased to 14 G, the rf power lowered to 700 W, and the flow rate increased to 8.6 sccm; yielding pressures in the source and expansion regions of 1.0 mTorr and 0.09 mTorr, respectively.

Shown in Fig. 3 are the upstream LIF measurements of the IVDF versus rf frequency. Note that the rf frequency axis has been reversed compared to Fig. 1 so that the entire IVDF can be seen for each measurement. Because the laser injection direction is also reversed, a negative frequency shift corresponds to ion flow towards the expansion chamber for these data. After correcting for Zeeman shifts there is a slight increase in the downstream drift velocity of the bulk ion population with increasing antenna frequency, from 6.7 km/ sec at 9.5 MHz to 7.5 km/ sec at 12 MHz. Note that for antenna frequencies below 11.5 MHz, a broad tail of slower ions appears. By 9.5 MHz, the tail of slow ions expands to include ions moving in the upstream direction as well. The increase in beam velocity with increasing antenna frequency is opposite to what was observed in the downstream measurements. To confirm that at these slightly different parameters the plasma exhibited the same phenomena as was shown in Figs. 1 and 2, the downstream IVDF was monitored with a RFEA probe during the antenna frequency scan. The RFEA measurements confirmed that an ion beam appeared downstream only for frequencies above 12 MHz. Thus, the broad tail of slower ions in the upstream IVDF also only appears when the DL forms in the expansion region.

During these experiments, it was noticed that the upstream and downstream Langmuir probe measurements were extraordinarily noisy for antenna frequencies up to 11.5 MHz. Each measurement had to be repeated many times to obtain reliable density and electron temperature measurements. Above frequencies of 12 MHz, a single measurement was sufficient. To quantify this phenomenon, the average root-mean-squared deviation from a linear fit to a 6.0 V wide region of the Langmuir probe *I-V* curve in the electron retardation region [17] was calculated as a function of antenna frequency and the results of the analysis, normalized to the average value of the reference *I-V* curve in that same region, are shown in Fig. 4. Essentially, Fig. 4 is a measure of the noise-to-signal versus rf frequency. These data indicate that coincident with the appearance of the current-free DL, there is a dramatic reduction in the electrostatic noise both upstream and downstream of the expansion region. The frequency spectrum of the fluctuations at an antenna frequency of 11.5 MHz, as measured with a two-tip, electrostatic probe, is shown as an inset in Fig. 4. The fluctuations are dominated by a wave at a fundamental frequency of 17.8 kHz and its harmonics. The wave propagates primarily in the axial direction (so it is not a drift wave) with an axial wavelength of approximately 2 cm. The short parallel wavelength and multiharmonic excitation are inconsistent with the characteristics of the ionization instability observed in another DL experiment [18].

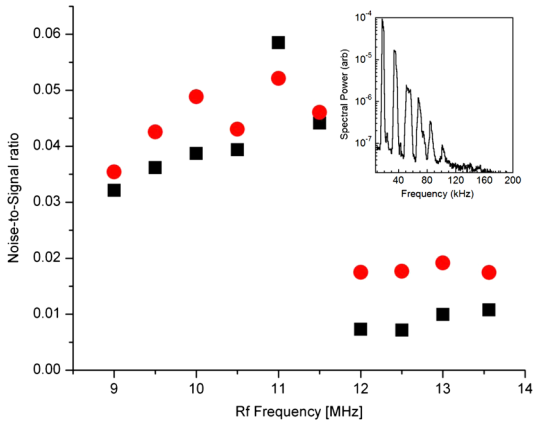

FIG. 4 (color online). Upstream (squares) and downstream (circles) noise-to-signal ratio versus antenna frequency. The inset shows a typical frequency spectrum of the fluctuations.

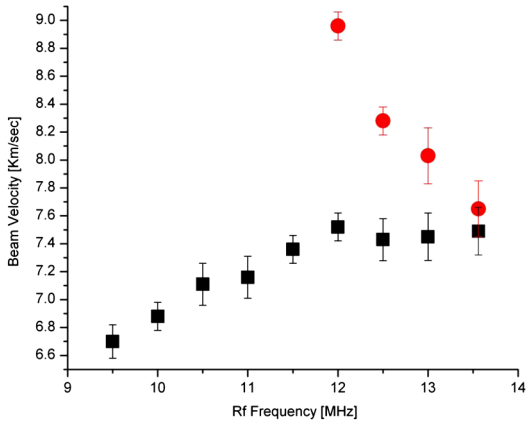

FIG. 5 (color online). Upstream (squares) and downstream (circles) ion beam velocity versus antenna frequency. Note that the upstream data is for an expansion magnetic field strength of 14 G while the downstream data is for an expansion field of 50 G.

Based on the increase in the upstream ion flow speed into the DL region as the antenna frequency decreases from 13.56 MHz, we suggest the following interpretation. At antenna frequencies below 12 MHz, a strong DL attempts to form. The accelerated ion and electron beam currents exceed a current threshold, because of the increasing inflow speeds, and electrostatic instabilities large enough to disrupt DL formation develop. The instabilities appear as large amplitude noise on the Langmuir probe and RFEA measurements. Because the double layer is unstable, the upstream ions are not continuously accelerated towards the expansion region and a broad ion population, consisting of an accelerated bulk population and a long tail extending down to rest energies, results (see Fig. 3). The upstream bulk ion speeds and the downstream ion-beam speeds extracted from the LIF data shown in Figs. 1 and 3 are shown in Fig. 5. The downstream ion-beam velocity clearly increases with decreasing antenna frequency until the beam abruptly vanishes downstream, i.e., the DL is getting stronger before it vanishes (and therefore the net current through the DL is increasing). The upstream beam velocity is relatively constant at the higher antenna frequencies and then begins to drop at the same threshold frequency for which the downstream ion beam vanishes. The increase in DL strength with decreasing antenna frequency is probably related to the modest improvement in rf coupling at lower antenna frequencies seen previously in this experimental system [19]. Note that significantly improved rf coupling with decreasing frequency would result in larger densities at lower frequencies; contrary to what is observed in these experiments.

Because the appearance of this instability disrupts DL formation, these measurements provide a unique means of confirming the theoretical prediction that formation of a current-free DL in an expanding plasma results in increased upstream ionization. Thus, DL formation very likely arises out of a need to balance upstream and downstream losses and should occur in any, low pressure, expanding plasma. The characteristics of the instability: multiple harmonics spanning frequencies below and above the ion cyclotron frequency; wavelengths much shorter than the system size and some tens of times larger than the Debye length; parallel propagation; and association with a threshold in particle drift velocity comparable to the ion sound speed ($\sim$7 km/s for these plasmas), point to an electrostatic ion-ion acoustic instability [20].

Work supported by NSF Grant No. PHY-0611571.

[1] C. Charles and R. W. Boswell, Appl. Phys. Lett. **82**, 1356 (2003).
[2] S. A. Cohen *et al.*, Phys. Plasmas **10**, 2593 (2003).
[3] X. Sun *et al.*, Phys. Rev. Lett. **95**, 025004 (2005).
[4] C. Charles *et al.*, Phys. Plasmas **7**, 5232 (2000).
[5] Z. Harvey *et al.*, Rev. Sci. Instrum. **79**, 10F314 (2008).
[6] L. P. Block, Astrophys. Space Sci. **55**, 59 (1978).
[7] C. Charles and R. W. Boswell, Appl. Phys. Lett. **91**, 201505 (2007).
[8] F. W. Perkins and Y. C. Sun, Phys. Rev. Lett. **46**, 115 (1981).
[9] M. A. Lieberman *et al.*, J. Phys. D **39**, 3294 (2006).
[10] M. A. Lieberman and C. Charles, Phys. Rev. Lett. **97**, 045003 (2006).
[11] A. Fruchtman, Phys. Rev. Lett. **96**, 065002 (2006).
[12] I. D. Sudit and F. F. Chen, Plasma Sources Sci. Technol. **3**, 162 (1994).
[13] C. Biloiu *et al.*, Rev. Sci. Instrum. **75**, 4296 (2004).
[14] E. E. Scime *et al.*, Plasma Sources Sci. Technol. **7**, 186 (1998).
[15] G. D. Severn *et al.*, Rev. Sci. Instrum. **69**, 10 (1998).
[16] R. F. Boivin and E. E. Scime, Rev. Sci. Instrum. **74**, 4352 (2003).
[17] I. H. Hutchinson, *Principles of Plasma Diagnostics* (Cambridge University Press, Cambridge, England, 1987).
[18] A. Aanesland *et al.*, Phys. Rev. Lett. **97**, 075003 (2006).
[19] P. A. Keiter *et al.*, Phys. Plasmas **4**, 2741 (1997).
[20] S. P. Gary and N. Omidi, J. Plasma Phys. **37**, 45 (1987).